Clustering and Protein Dynamics of *Drosophila melanogaster* Telomeres

Natalia Wesolowska,*,†,1 Flavia L. Amariei,*,2 and Yikang S. Rong*,1

*Laboratory of Biochemistry and Molecular Biology, National Cancer Institute, National Institutes of Health, Bethesda, Maryland 20892 and †National Institutes of Health and Johns Hopkins University Graduate Partnership Program, Bethesda, Maryland 20892

ABSTRACT Telomeres are obligatory chromosomal landmarks that demarcate the ends of linear chromosomes to distinguish them from broken ends and can also serve to organize the genome. In both budding and fission yeast, they cluster at the periphery of the nucleus, potentially to establish a compartment of silent chromatin. To gain insight into telomere organization in higher organisms, we investigated their distribution in interphase nuclei of *Drosophila melanogaster*. We focused on the syncytial blastoderm, an excellent developmental stage for live imaging due to the synchronous division of the nuclei at this time. We followed the EGFP-labeled telomeric protein HOAP *in vivo* and found that the 16 telomeres yield four to six foci per nucleus, indicative of clustering. Furthermore, we confirmed clustering in other somatic tissues. Importantly, we observed that HOAP signal intensity in the clusters increases in interphase, potentially due to loading of HOAP to newly replicated telomeres. To determine the rules governing clustering, we used *in vivo* imaging and fluorescence *in situ* hybridization to test several predictions. First, we inspected mutant embryos that develop as haploids and found that clustering is not mediated by associations between homologs. Second, we probed specifically for a telomere of novel sequence and found strong evidence against DNA sequence identity and homology as critical factors. Third, we ruled out predominance of intrachromosomal interactions by marking both ends of a chromosome. Based on these results, we propose that clustering is independent of sequence and is likely maintained by an as yet undetermined factor.

TELOMERE DNA is shaped into a protective configuration by protein complexes whose function is to distinguish these natural ends from DNA double-strand breaks (DSBs). Telomeres are also universal structures of all linear chromosomes and constitute nuclear bodies and, as such, they exhibit specific nuclear compartmentalization and protein dynamics. Both of these aspects of telomere behavior have not been thoroughly investigated.

The best-known example of the role of telomeres in nuclear organization is in the formation of the bouquet configuration of meiotic prophase chromosomes, observed in a wide range of organisms and thought to facilitate pairing of homologous chromosomes (reviewed in Scherthan 2001). Here, telomeres cluster together and initiate contacts between homologs. This level of chromosome organization, which guarantees faithful segregation of homologs, is specialized for sexual reproduction. In contrast, the contribution of telomeres to organization in somatic tissues is often implied, but not well understood. In *Saccharomyces cerevisiae*, telomere organization in mitotic interphase is as striking as that in meiosis, with the 32 telomeres of the haploid clustering in three to eight groups at the nuclear periphery (Palladino *et al.* 1993; Gotta *et al.* 1996; Laroche *et al.* 1998; Taddei and Gasser 2004). Telomeres in *S. cerevisiae* are hubs for silent information regulators (SIRs), which nucleate heterochromatin. Telomere clustering is thought to create a protective sink that sequesters SIRs away from the rest of the genome (Taddei *et al.* 2009). A similar organization of telomeres has also been observed for the distant fungus *Schizosaccharomyces pombe* (Chikashige *et al.* 2009; Fujita *et al.* 2012).

Studies in animals and plants have revealed that telomere positioning in higher organisms is usually not peripheral (Manuelidis 1984; Ferguson and Ward 1992; Vourc'h *et al.* 1993; Dong and Jiang 1998) but might still be confined by the nuclear matrix (De Lange 1992; Pierron and Puvion-Dutilleul 1999; Weipoltshammer *et al.* 1999). Telomere clustering, on the other hand, has been shown for different cell types (Billia and De Boni 1991; Nagele *et al.* 2001; Molenaar

doi: 10.1534/genetics.113.155408
Manuscript received June 3, 2013; accepted for publication July 19, 2013
Supporting information is available online at http://www.genetics.org/lookup/suppl/doi:10.1534/genetics.113.155408/-/DC1.
[1]Corresponding authors: Laboratory of Biochemistry and Molecular Biology, National Institutes of Health, 37 Convent Dr., Room 6056, Bethesda, MD 20892. E-mail: wesolown@mail.nih.gov; rongy@mail.nih.gov
[2]Present address: OriGene Technologies, Rockville, MD 20850.

et al. 2003; Ramirez and Surralles 2008) and might be an evolutionarily conserved nuclear feature. Very little is known about the mechanisms that cluster telomeres, although findings in *S. cerevisiae* reveal roles for the Ku heterodimer and Sir3 (Laroche *et al.* 1998; Gehlen *et al.* 2006; Ruault *et al.* 2011).

Another aspect of telomere nuclear bodies involves the dynamics of their associated proteins. As for any other region of chromatin, telomeres must "replicate" protein components alongside DNA with every cell cycle. For the bulk of chromatin, protein dynamics during replication are rapid. Nucleosomes reassemble immediately in the tracks of the progressing fork (reviewed in Groth *et al.* 2007). Centromeres, on the other hand, exhibit stage-specific reloading with the exact timing differing, depending on the organism or tissue (Jansen *et al.* 2007; Schuh *et al.* 2007; Mellone *et al.* 2011). Analogously, as the protein component present at telomeres is presumably redistributed to the two chromatids, complete telomeres must be reestablished with loading of new protein.

Here, we aimed to elucidate two areas of telomere biology: first, the organization of telomeres and, second, the dynamics of telomeric proteins during interphase. We focused our attention on the syncytial blastoderm for this analysis. At this stage the nuclei progress synchronously through the cell cycle within a monolayer at the embryo periphery, providing a perfect milieu for imaging of nuclear dynamics. We found that during interphase in the embryo, the 16 telomeres clustered into four to six foci in a polarized manner that is consistent with previously reported Rabl organization of the nucleus (Hiraoka *et al.* 1990). We found that telomere clusters exhibited doubling of HOAP intensity during interphase—dynamics that could be indicative of protein loading. Telomeres of other somatic tissues showed a level of clustering similar to that in the embryo. Furthermore, we investigated the contribution of three factors to clustering: (1) homolog interactions, (2) telomeric DNA identity or sequence homology, and (3) intrachromosomal interaction. We discovered that none of them play an essential role in maintaining clustering. Because clustering appears random among telomeres, we tested the role of some candidate proteins that could constitute a common mediator of clustering.

Materials and Methods

Drosophila stocks

EGFP-HOAP was generated by site-specific integrase mediated repeated targeting (SIRT) as discussed in Gao *et al.* (2011). The ms(3)k81 analysis was done on embryos from wild-type (wt) females mated to transheterozygous males of $ms(3)k81^{1}$ and $ms(3)k81^{2}$ mutants, both kindly provided by Barbara Wakimoto (University of Washington, Seattle). $mre11^{58S}$ and nbs^{2K} were described previously (Gao *et al.* 2009). Embryos for FISH analysis were collected from homozygous females mated to their siblings in the balanced stock. $Ku80^{KO}$ was generated by gene targeting by homologous recombination (ends out) and was confirmed via molecular assays (see schematic and test PCRs in Supporting Information, Figure S1). Embryos for FISH analysis were collected from the homozygous stock. The *klaroid* knockout w*; $koi^{HRKO80.w}$ (Bloomington 25105) was crossed into the EGFP-HOAP stock. Then, homozygous flies of w; $koi^{HRKO80.w}$; EGFP-HOAP were used for embryo collections. LacO stocks "LacO-int" with LacO array at 2L (36E) and "LacO3L" with the array at 3L (61F) were kindly provided by Lori Wallrath (University of Iowa, Iowa City, IA) and were previously described in Li *et al.* (2003).

Embryo and brain preparation for live imaging

EGFP-HOAP embryo collections were performed on grape juice plates for 2–2.5 hr. Embryos were dechorionated with 100% bleach for 45 sec and washed thoroughly with water. They were laid out horizontally on coverslip chambers (Lab-Tek, Chambered, coverglass system) and submerged in PBS for inverted-scope imaging. Only embryos at cycles 10–13, where the nuclei have migrated to the periphery, were used for imaging. For live brain imaging, brains of third instar larvae were dissected in PBS, placed on a coverslip in a drop of PBS, squashed gently by the weight of the slide lowered on top, and sealed for inverted-scope imaging.

Immunostaining

Immunostaining of larval tissue was performed according to the Rothwell and Sullivan protocol for embryo immunostaining (protocol 9.3 in Sullivan *et al.* 2000), disregarding the methanol dechorionation step. Antibody used for detection of HOAP was rabbit anti-HOAP.

Fluorescence in situ hybridization

Embryos were fixed according to the Rothwell and Sullivan protocol for embryo fixation (protocol 9.3 from Sullivan *et al.* 2000, *Drosophila Protocols*). Embryo FISH was performed according to the Dernburg protocol (Sullivan *et al.* 2000, Chap. 2), using TdT labeling to generate the probe from restriction enzyme-fragmented DNA (protocol 2.1–2.2) and the hybridization to tissue in liquid suspension (Sullivan *et al.* 2000, protocol 2.8). The plasmid DNA used for generation of the probe is a single copy of HeT-A sequence (GenBank sequence no. 01D09) inserted in pBluescript. The probe was detected using Rhodamine-conjugated anti-DIG antibody (Roche). LacO probes were manufactured as fluorescently labeled oligos LacOminusAlexa488, [AminoC6+Alexa488] CCACAAATTGTTATCCGCTCACAATTCCACATGTGG, and LacOplusCy3, [Cy5]CCACATGTGGAATTGTGAGCGGATAA CAATTTGTGG (Operon). Tissues were mounted in mounting media (Vectashield).

Confocal imaging and quantification

Most imaging was performed with the Zeiss510 confocal microscope (Carl Zeiss, Thornwood, NY), with a 63× oil immersion objective and a zoom of 4×. EGFP-HOAP and HeT-A FISH counts were performed for all images in a Z stack, for

five nuclei chosen at random per embryo. LacO distance analysis was done for image projections of a subset of Z sections. The distance in the z direction was not considered but most spot pairs were within the same Z section or separated only by one Z section (0.8 μm) and were only a small fraction of the distance considered. Measurements were done using ImageJ. Each measurement was normalized by dividing it by the average diameter of the nuclei in the embryo under consideration, determined from measurements of 10 nuclei.

HOAP intensity measurements

For analysis in Figure 3, Z stacks of embryos were taken every 2 min. After each stack, the stage was moved to a new point on the embryo, outside of the bleached square from the previous setting. No other parameters were altered between time points. Individual Z sections, containing best-focused images of the clusters, were selected for intensity measurements by photometry. Briefly, a total intensity of the circular region (aperture) encompassing a given telomere cluster was corrected for the average intensity of the surrounding background (annulus). The measurements were performed on original 8-bit TIFF image files with a "single-star photometry" tool in AIP4WIN software (AIP4WIN: http://www.willbell.com/aip4win/aip.htm). An inner aperture with a diameter of 7 pixels (480 nm) was sufficient to totally include a telomere cluster and an outer annulus with inner radius of 9 pixels and outer radius of 15 pixels (615 nm and 1025 nm, respectively) (see Figure S4) supplied the background intensity measurement. Fifteen foci were selected from each image at random for this analysis. Measurements were ranked using Excel software. Values were divided by the smallest measurement to normalize the signal.

Statistics

The nonparametric Mann–Whitney test was used as the statistical test for significance performed with InStat software and is reported as a two-tailed *P*-value in the text.

Results and Discussion

Telomeres cluster in the syncytial blastoderm

To observe and follow the organization of telomeres, we inserted the EGFP tag sequence at the 5′ end of the endogenous HOAP gene (*caravaggio*). Flies expressing the N-terminal fusion EGFP-HOAP showed no discernible telomere phenotypes, and EGFP-HOAP protein levels appeared close to endogenous on a Western blot (Figure S2). We confirmed that *in vivo*, EGFP-HOAP localizes to telomeres of polytene nuclei in salivary glands (not shown) and to anaphase telomeres in syncytial blastoderm nuclei (Figure 1C). Additionally, HOAP antibody staining in fixed tissues (Figure S3A, third panel) colocalizes with EGFP fluorescence (Figure S3A, fourth panel). Therefore, we conclude that EGFP-HOAP is a valid maker for determining telomere position and movement in the *Drosophila* nucleus.

A 10- to 15-μm confocal Z stack of images from the surface to the interior of the embryo at ~2 hr of development allows for the observation of telomere signal within the layer of nuclei. Bright EGFP foci are visible above the dim nuclear background (Figure 1B). We performed counts of these foci within 100 nuclei (across 20 different Z stacks, collected from 12 embryos) and determined that on average there are 4–6 foci per nucleus, with a mean of 5.3 (standard deviation 1.3, Figure 1D), strongly suggesting that the 16 telomeres of the diploid are in clusters (sister chromatids are assumed to remain together, as shown in Fung *et al.* 1998).

We observed a polarized foci distribution in the nucleus, consistent with Rabl configuration (Hiraoka *et al.* 1990). This is shown in the representative panels in Figure 1B. The telomeres of the fourth "dot" chromosome and the short-arm telomere of the acrocentric X chromosome likely occupy the same nuclear region as the centromeres and would be found on top, potentially clustering into the one to two foci visible in the top panel. Most of the telomeres of the other chromosomes are situated at the ends of long chromosomal arms and reach down to the bottom of the nucleus where they would cluster in two to four foci, leaving the middle devoid of foci. The model is drawn to suggest that the telomeres of each chromosome (and its homolog) cluster among each other (Figure 1B), as proposed previously (Hiraoka *et al.* 1990).

An additional aspect of the syncytial blastoderm that makes it especially advantageous for looking at telomere clustering is that homolog pairing does not occur until later cycles. Homolog pairing, in which homologs are associated along their length, dominates the *Drosophila* mitotic organization of chromosomes in the soma (McKee 2004), but the process is not established until after cycle 14 (Fung *et al.* 1998). Hence, the clustering results for cycles 9–13 are not compounded by chromosome interactions due to homolog pairing. Nonetheless, the peculiar nature of the syncytium might also be seen as untranslatable to other cell types. To determine whether clustering is a universal characteristic of mitotic interphase, we set out to determine whether telomeres cluster in other somatic tissues.

Telomeres cluster in other Drosophila somatic tissues

Observation of nuclei in whole-mount preparations of live third instar larval brains from EGFP-HOAP flies revealed a signal distribution comparable with that in the embryo. Figure S3B shows an example image, in which the cell contours are visible under the DIC illumination. In average-sized nuclei we observed 4–6 EGFP foci, with a mean of 5.16 (SD = 1.37, $n = 38$, from five brains, Figure 1E), which was not significantly different from that observed in the embryo ($P = 0.48$). If the only constraint was homolog pairing, the 16 telomeres should be "clustered" in eight pairs (or 7 foci, if the telomeres of the fourth chromosome cannot be discerned). This number is substantially larger than the number of foci we observed. However, we also noted larger cells with ~6–8 foci per nucleus ($n = 12$). We speculate that

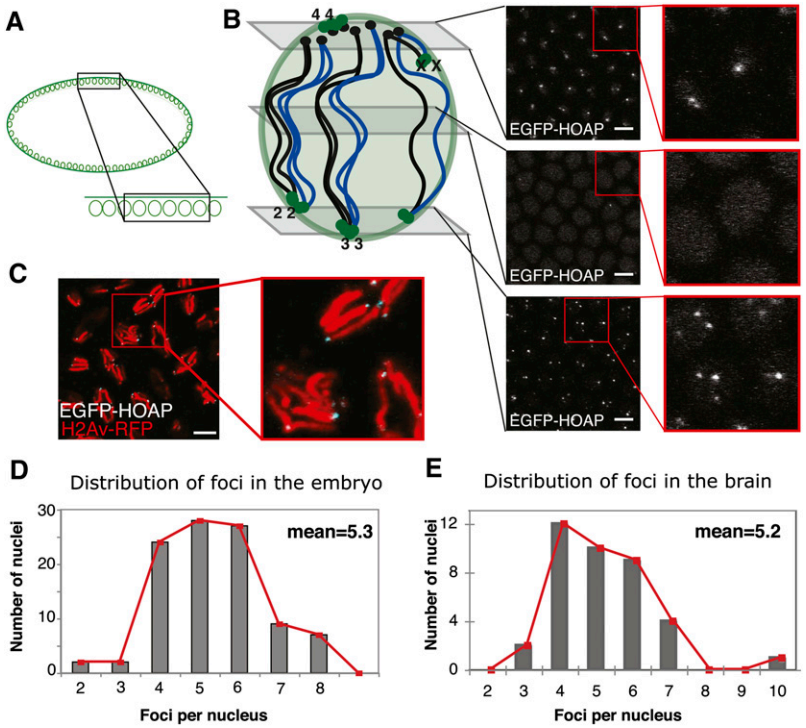

Figure 1 The distribution of telomere foci numbers. (A) Schematic of a side view of an embryo with a "zoomed-in" section for the confocal images in B, where it is viewed from the top. (B) Representative images from a Z stack taken in EGFP-HOAP embryos, with approximate positions along the vertical axis indicated on the schematic representation on the left. Schematic shows a polarized syncytial nucleus: black circles are centromeres, green circles are telomeres, and black and blue lines connecting the two are the chromosomal arms, with the two colors representing the two homologs. Right, images are confocal sections from a Z stack, with a zoom-in of the area in the red square and EGFP-HOAP signal in white. (C) Image from a confocal Z stack of embryos in mitosis, with a zoom-in of the area in the red square. H2Av-RFP is in red, and EGFP-HOAP is in white. (D) Histogram of telomere foci numbers from 100 nuclei in the syncytial blastoderm (from 13 embryos). Mean of the distribution is shown. (E) Histogram of telomere foci distribution from 40 nuclei (from three larval brains). Red line is a trace of bar plot values; mean of the distribution is shown. Bars for all, 5 μm.

these cells might be premitotic, and chromosome condensation and alignment at metaphase might disrupt the clusters. With the exception of these cells, our results confirm that telomeres are also clustered in the larval brains and suggest that clustering occurs to the same extent in different *Drosophila* tissues.

HOAP dynamics at the telomere

We observed that the EGFP-HOAP signal changed throughout interphase—indicative of telomere protein dynamics. To elucidate these dynamics, we made use of H2Av-mRFP, a histone variant marker, to follow the progression of the cycle in the EGFP-HOAP flies. Figure 2 shows a time-lapse series taken within a single embryo with 2-min intervals. Each Z section comes from a Z stack taken at the indicated time point (in panels labeled from tp-0min to tp-18min). Chromatin organization can be deduced from the red histone signal. The anaphase images show that tp-8min and tp-10min capture mitosis (see circled anaphase figures), allowing deduction of cell cycle stages in the other panels (as indicated on top of the panels).

EGFP signal alone is shown in the middle panels of the top and bottom sections of Figure 2, whereas the bottom panels show zoomed-in images for clarity. A qualitative inspection of EGFP signal in this time-lapse series allowed us to draw some preliminary conclusions about the dynamics of HOAP. In interphase, EGFP-HOAP formed bright foci, as can be seen from the examples indicated within tp-0min for each of the three panels (green arrowheads). These foci became brighter as interphase proceeded (compare foci indicated with yellow arrows in tp-12min, tp-14min, tp-16min, and tp-18min). Throughout interphase, HOAP also showed a nuclear background, which disappeared at the onset of mitosis (starting at tp-4min). It reappeared at the next interphase (tp-12min) and became more pronounced with time. This background signal does not appear to be exclusively chromatin associated, as can be inferred from tp-2min. Whereas histone-RFP shows distinct chromosomal shapes at this time, the background EGFP-HOAP still looks uniform throughout the nuclear space (Figure 2). According to our observations, telomeres were separate at anaphase, but exhibited clustering right at the onset of interphase (tp-12min).

Because the homozygous H2Av-mRFP flies exhibited some mitotic perturbation, we decided to perform the quantification analysis for HOAP signals without the histone marker. We also took advantage of our system to avoid bleaching throughout the time-lapse series. For each time point, we moved down the length of the embryo, so that each Z stack captured fresh nuclei, not yet exposed to imaging. Because they belong to the same animal and are synchronized, the nuclei from different time points were treated as "the same" sample.

The changes in HOAP occupancy at telomere clusters were quantified by photometric intensity measurements. For each time point, we chose a Z section that had the strongest telomere signal. Intensity of foci was measured with a set aperture size and adjusted for background intensity (see adjustment in Figure S4). To determine changes in HOAP telomere occupancy from one time point to the next, we measured the fluorescence intensity of 15 randomly chosen foci for each image. This provided a distribution of signals for each time point. To compare only the clusters constituting

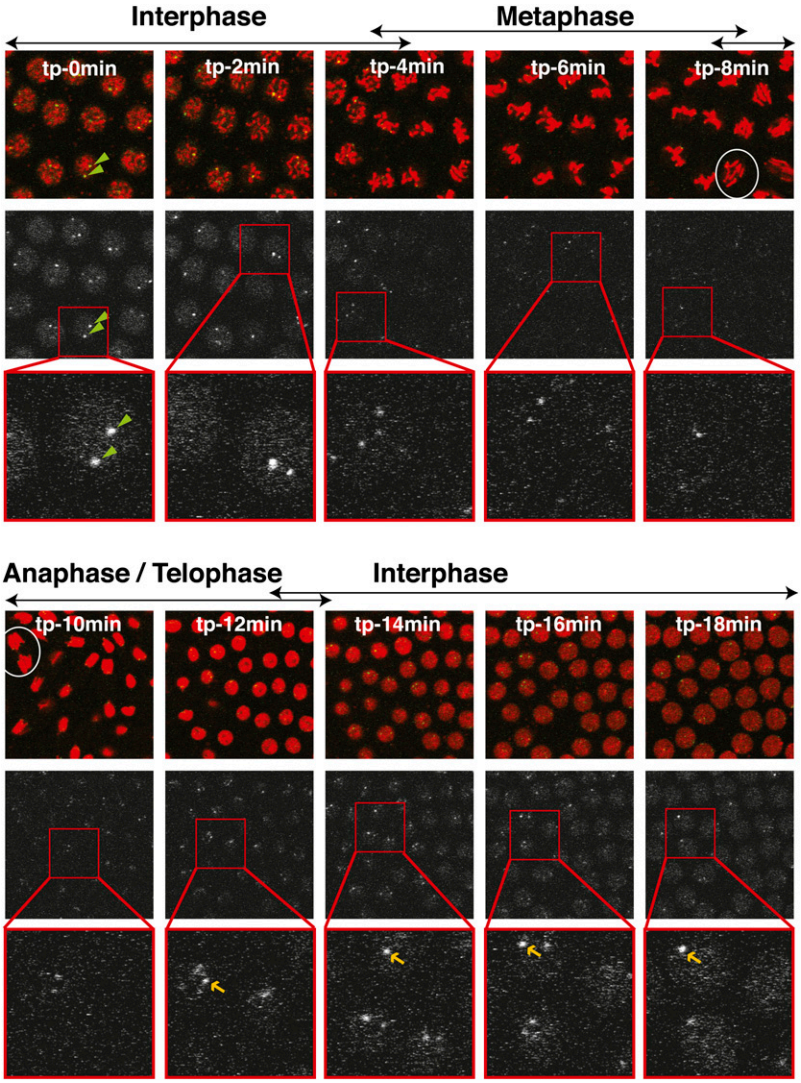

Figure 2 Telomere signal throughout the cell cycle. Panels represent a time-lapse series in a syncytial blastoderm embryo. Each time point, labeled with its corresponding time (from tp-0min to tp-18min), shows three panels: top, merged image of EGFP-HOAP (green) and H2Av-mRFP (red); middle, EGFP-HOAP signal alone (white); and bottom, zoom-in of the EGFP signal from the area in the red square from the middle panel. Cell cycle stages deduced from chromatin characteristics are shown above the merged image. Green arrowheads within panels for tp-0min point to two telomeric foci. White ovals label two anaphase figures (tp-8min and tp-10min). Yellow arrows point out the telomeric foci that allow one to observe the increase of telomeric signal over time (from tp-12min to tp-18min).

a similar number of telomeres, we organized the distributions by ranking (Nagele *et al.* 2001). The graph in Figure 3A shows individual measurements for embryo 1, which are represented by bars of different shades of gray, ranked from largest to smallest for each time point.

Time-point comparisons revealed an increase in intensity across all tiers from early to late distributions (compare open to solid bars in Figure 3A). This might suggest that as interphase proceeds, additional protein is loaded on telomeres, resulting in an increase in HOAP signal. Figure 3B shows a similar series for "embryo 2", which recapitulated what we observed with embryo 1. The series started early in interphase, as inferred from the faint nuclear background in tp-0min, and proceeded through late interphase (tp-6min), where again the intensity values approximately doubled across the ranking. Similar results were observed for series taken from additional three embryos.

Our observations that HOAP signal increased during interphase indicate that loading of HOAP to telomeres might occur during interphase. Furthermore, they suggest that a full telomeric cap might be restored concurrent with telomere replication.

Different mechanisms governing telomere clustering

To investigate the mechanisms governing telomere clustering in *Drosophila*, we put forth three specific hypotheses (see models in Figures 4A, 5A, and 6A). First, we considered that a major contributor to clustering might be the pairing of homologous chromosomes, even if only at the telomeric regions; second, we posited that clustering might be a result of DNA sequence homology; third, we explored whether it could be a result of intrachromosomal interaction, *i.e.*, association of telomeres of the same chromosome. We discuss our exploration of these three hypotheses within the syncytial blastoderm in the following sections.

Telomere clustering is not mediated by homolog pairing: It has been previously suggested that the telomeres of homologs interact with each other in syncytial blastoderm embryos (Hiraoka *et al.* 1990). Despite the fact that

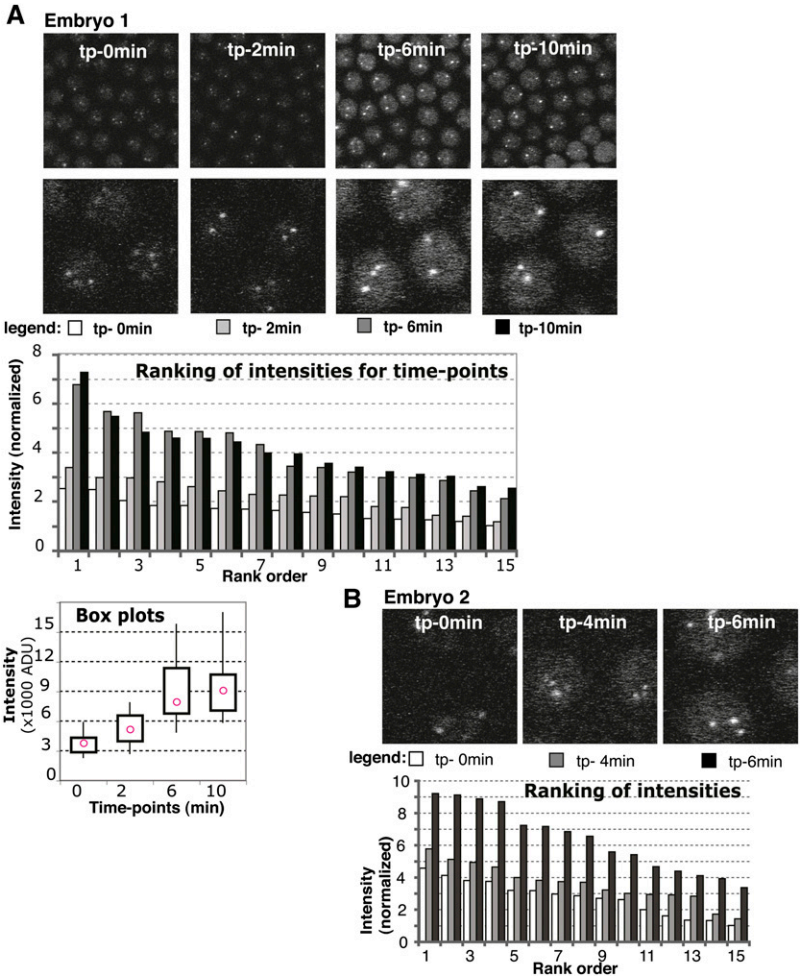

Figure 3 Time-lapse series analysis of EGFP signal. (A) Embryo 1 intensity distributions. (Top) Panels used for measurements are shown for each time point with zoom-in below. Time points (tp) are indicated within the top panel. (Bottom) Ranking graph: data for each time point were ranked and represented with different shades of gray as indicated in the legend underneath the images for each time point. *y*-axis: intensity is normalized to the smallest intensity value from the whole series (set to 1). Box plots graph: intensity distribution for each time point with pink circles showing the median value. *x*-axis: time point. *y*-axis: intensity, actual values [in thousands of arbitrary densitometric units (ADU)]. The boxes contain data between the first and third quartiles, while whiskers extend to minimum and maximum. (B) Zoomed-in images and ranking graph for embryo 2, presented as in A.

homolog pairing is not yet established at this stage (Fung *et al.* 1998), we considered that the telomeres of homologs might already be paired and precede the process (Figure 4A, hypothesis 1).

To determine whether clustering is a consequence of homolog interactions, we observed telomere organization in the nuclei of "haploid embryos" fathered by *ms(3)k81*. The *ms(3)k81* mutant exhibits a paternal lethal phenotype, presumably due to failure to establish telomeres in the paternal pronucleus after decondensation (Dubruille *et al.* 2010; Gao *et al.* 2011). Paternal chromosomes suffer telomere fusions and are subsequently eliminated, resulting in embryos that develop as maternal haploids through the syncytial blastoderm stage. If the hypothesis that clustering is a result of homolog interaction were correct, then in the haploid embryos, where one of the sets of homologs is absent, clustering would be diminished. In actuality, we observed fewer but just as intense telomere foci with an average of 3.4 (SD = 1.5; see Figure 4B for an example confocal projection and Figure 4C for distribution of foci in 44 nuclei, across nine embryos). This result suggests that telomeres still cluster in the absence of the homologous chromosomes and provides evidence against our first hypothesis.

Clustering does not require sequence homology: Another hypothesis is that clustering is mediated by the homology of DNA sequences at telomeres (Figure 5A, hypothesis 2). *Drosophila* telomeres are not composed of the classical telomerase-synthesized repeats, but rather of retrotransposons that specifically target the chromosomal ends (Silva-Sousa *et al.* 2010). The repetitive terminal sequences provide broad regions of homology between telomeres. Assuming hypothesis 2 is true, a telomere whose natural sequences are replaced with a unique sequence would lose its ability to cluster. Because telomere-capping function in the fly is independent of sequence and a novel telomere can be established on any terminal DNA (Biessmann and Mason 1988; Levis 1989; Beaucher *et al.* 2012), we were in a position to test this hypothesis. We generated a telomere at chromosome 3R that lacked native telomeric DNA and instead consisted of an array of ~240 copies of the lac "operator" sequence (lacO) from bacteria (L. Zhang, M. Beaucher, Y. Cheng, and Y. S. Rong, unpublished data). We named this lacO-marked telomere LacO3R-TD. We note here that it is formally possible that between the time of establishing the TD line and the time of the experiment (~1 year), the stock could acquire a retrotransposon copy at that end. Nonetheless, this is very unlikely as attachment of new elements at

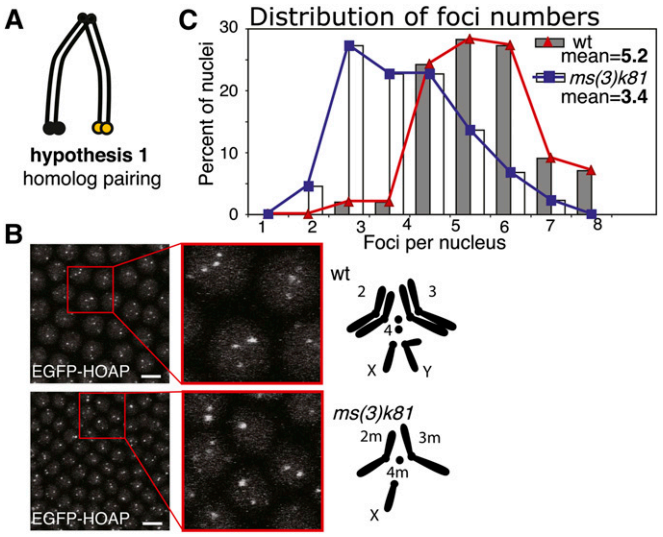

Figure 4 Test of homolog pairing as a determinant of clustering. (A) Schematic for hypothesis 1, homolog pairing. (B) EGFP-HOAP foci in wt and a haploid embryo; left, confocal projection, with a zoom-in; right, schematic of chromosomes for wt (top) and *ms(3)k81* mutant (bottom) as indicated. Bar, 5 μm. (C) A histogram of telomere count distribution from wt (same as the one shown in Figure 1), represented by gray bars and red line, and from *ms(3)k81*, represented by white bars and blue line (44 nuclei). Means are shown within the graph.

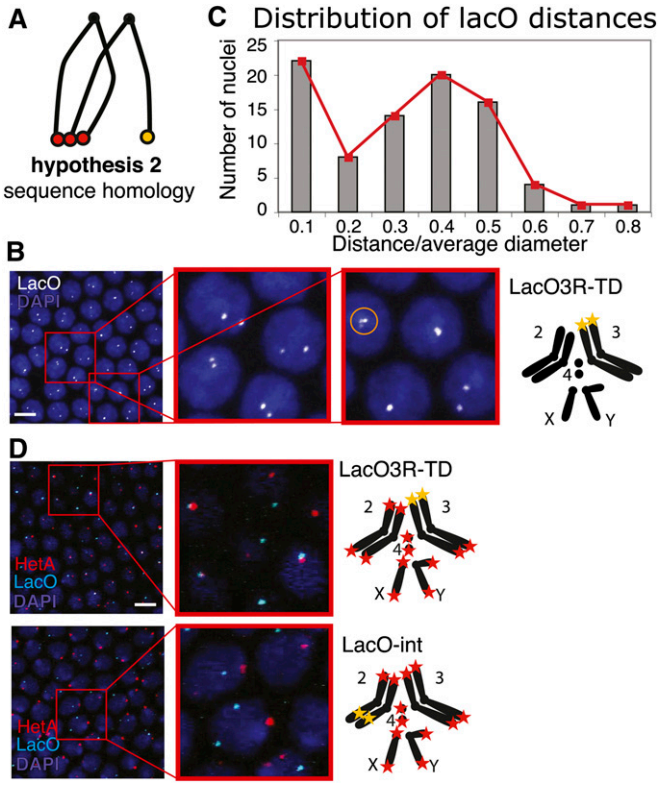

Figure 5 Test of sequence homology as a determinant of clustering. (A) Schematic for hypothesis 2, sequence homology. (B) Pairing of LacO telomeres. Left, confocal projection of LacO FISH, with two zoom-ins, LacO probe in white, DAPI in blue. Right, genotype and schematic of chromosomes for LacO3R-TD. Telomere 3R is replaced by the LacO array, and LacO is visualized with a LacO probe (yellow star). Sometimes we observed more than two foci in a nucleus (see circled cluster of three foci in second zoom-in). We assume that those were instances where the replicated sister telomeres separated from each other. (C) Histogram of distance between the two LacO signals (n = 85 nuclei, from three embryos). Distance has been normalized by dividing by the average size of the nuclear diameter. (D) Interaction of LacO telomere with retrotransposon telomeres. Left, confocal projections of LacO and HeT-A FISH, with a zoom-in, HeT-A in red, LacO in cyan, and DAPI in blue. Right, genotypes and schematics of chromosomes for LacO3R-TD (top) and LacO-int (bottom). Bars for all, 5 μm.

the TD is rare (0.1% per generation, *e.g.*, in Beaucher *et al.* 2012), and our molecular analysis of the end over time has never revealed such additions to the LacO-sequence telomere (N. Golenberg, F. L. Amariei, and Y. S. Rong, unpublished data).

Embryos homozygous for the LacO3R-TD were used to observe the clustering of the sequence-unique telomere both with a homologous partner and with heterologous partners (*i.e.*, the transposon-comprised telomeres). Both types of telomere were visualized by FISH. For LacO3R-TD, we used a probe to LacO. Consistent with the Rabl orientation (as is illustrated in Figure 1B), the LacO signal at 3R was found within the bottom third of the Z stack. To follow the transposon telomeres, we used a probe that recognizes the sequence of the most abundant telomeric retrotransposon, HeT-A.

First, we investigated the LacO3R-TD's ability to cluster with its homolog (LacO–LacO clustering). An example projection of a FISH image is shown in Figure 5B, whereas Figure 5C shows the distribution of distances between the two foci. When we encountered a single focus, presumably from overlapping foci, distance was represented by the diameter of the focus. All measurements were normalized by dividing distance by an average nuclear diameter. About 25% of the foci fall in the first bin (22 of the total of 86 pairs analyzed, from three embryos). This spike in the distribution at the shortest distance confirms that close proximity of LacO signals is not accidental or the result of a temporary colocalization, but rather represents true clustering. Thus, one-fourth of the nuclei showed the two LacO foci clustered into a single focus.

To further interpret these results, we calculated the expected probability of clustering for any two telomeres of long-arm chromosomes. These telomeres formed two to four clusters at the bottom of the nucleus, with an average of three. Two telomeres treated identically can assume nine different configurations within three clusters (the first telomere has three positions it can claim, as does the second telomere; therefore there are $3 \times 3 = 9$ combinations). For three of these configurations, both telomeres under consideration are within the same cluster. Thus, we would expect 33% (3/9) of nuclei to show the two telomeres as clustering. The 25% of LacO/LacO colocalization suggests that clustering of homologous telomeres is not favored over random cluster occupancy.

Heterologous interactions occurred frequently (Figure 5D, LacO3R-TD). Approximately 63% of the 40 LacO foci

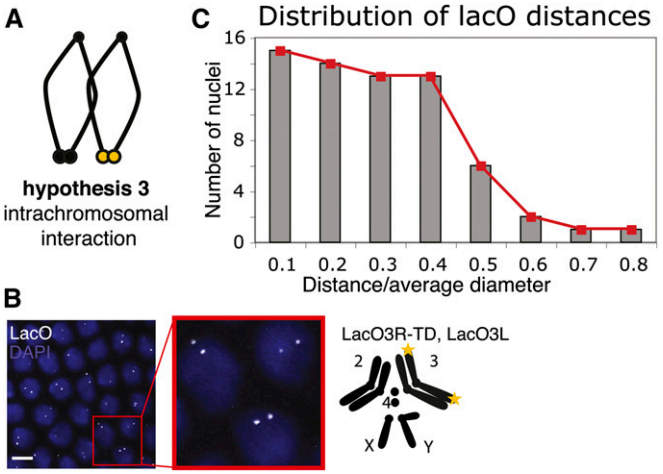

Figure 6 Test of intrachromosomal interaction as a determinant of clustering. (A) Schematic for hypothesis 3, intrachromosomal interaction. (B) Pairing of chromosome 3 telomeres. Left, confocal projection of LacO FISH, with a zoom-in, LacO probe in white, DAPI in blue. Right, genotype and schematic of chromosomes: telomere 3R is replaced by a LacO array and telomere 3L is marked by a subtelomeric LacO array; both are visualized with a LacO probe (yellow stars). Bar, 5 μm. (C) A histogram of distance between the two LacO signals (n = 65 nuclei, from four embryos). Distance has been normalized as in Figure 5B.

analyzed (in 38 nuclei) showed colocalization with HeT-A. This is not surprising if we consider that there are more heterologous partners for the LacO telomere to pair with. It does, however, indicate that there is no barrier to telomere clustering in the case of sequence heterology. On the other hand, in a similar experiment done with an internal LacO array within 2L (at cytological location 36E), termed LacO-int, none of the 54 LacO foci analyzed (in 37 nuclei) showed colocalization with the HeT-A signal, despite the fact that both were frequently within the same Z section (Figure 5D, LacO-int). This control rules out the possibility that the LacO sequence can induce clustering.

This result indicates that homology is not a strong determinant for telomere clustering and serves as evidence against hypothesis 2. The transposon telomere sequence in *Drosophila* appears dispensable for clustering, just as it is for telomere capping. Furthermore, this analysis provides support for rejection of the homolog-pairing hypothesis in the previous section, as the two LacO3R-TD telomeres showed no preference for clustering with each other. And, importantly, capture of the heterologous interaction, which revealed two different telomeres touching each other, should alleviate any doubts about the reality of telomere clustering that might have remained from our *in vivo* analysis.

These findings have implications for the suggestion that telomere clustering is a result of recombination. In the case of *Plasmodium*, telomere clustering is presumed to be a consequence of recombination between the genes in the terminal chromosome regions, a phenomenon significant for the virulence of the organism (Scherf *et al.* 2008). The transience of telomere associations in human cell culture (on the order of minutes) was also thought to be symptomatic of recombination (Molenaar *et al.* 2003). Here we present evidence that in *Drosophila*, homology in the telomeric sequences is not necessary for clustering.

Clustering is not a result of intrachromosomal telomere interaction: Our third hypothesis for clustering preferences posits that clusters are predominantly interactions of the telomeres of the same chromosome, *i.e.*, intrachromosomal interactions (Figure 6A, hypothesis 3). This hypothesis finds support in experiments from mammalian cell culture, where Daniel and St. Heaps (2004) found that probing for both subtelomeres of a single chromosome revealed their proximity in noncycling (G1), but not in cycling lymphocytes. From investigation of the preferred composition of clusters and detailed telomere-swapping experiments in yeast, Schober *et al.* (2008) also concluded that equal-length chromosomal arms (3L/3R and 6L/6R) exhibit a preference for clustering with each other. They reasoned that those telomeres are poised for contact at anaphase when chromatids pull apart, and this initial interaction is preserved throughout interphase.

To test the prevalence of intrachromosomal interaction, we marked both telomeres of the same chromosome. We utilized a subtelomeric LacO insertion at cytological position 61F, to mark the end of chromosome 3L. This LacO3L was recombined onto LacO3R-TD to achieve simultaneous marking of 3L and 3R telomeres. This time we conducted FISH analysis in heterozygous embryos so that we would follow the telomeres of only one of the two chromosome 3 homologs. To obtain heterozygous embryos, we crossed homozygous males to wt females. An example projection of a FISH image is shown in Figure 6B. Here again the telomeric signals appear in the bottom third of the Z stack in the polarized nucleus. We quantified the interaction of the two signals according to their distance (Figure 6C, 65 nuclei, from four embryos), as in Figure 5C. A distribution skewed toward short distances would indicate clustering of the opposite telomeres into one focus. Since LacO3L is nontelomeric, clustering would bring the two signals only into proximity of each other, rather than into a single spot. This could explain why both the 0.1- and 0.2-bin positions in the histogram have high occupancy. Only 15 pairs fell within the 0.1 bin, *i.e.*, 23%. Our results indicate that in the case of the *Drosophila* embryonic nucleus, the looped intrachromosomal interaction is not predominant.

The analysis from the above three sections does not support any of the three hypotheses we put forth at the outset. We conclude that clustering is likely to be indiscriminant among the telomeres that occupy the same Z position in the nucleus. We propose that the interactions among telomeres are mediated by factors that are present at all ends, regardless of their identity. Ruault *et al.* (2011) provided some evidence for this scenario, demonstrating that Sir3 overexpression enhanced the level of clustering in the nucleus. They suggest that initial interaction of telomeres at anaphase might be established by oligomerization of telomeric Sir3 from different chromosomes.

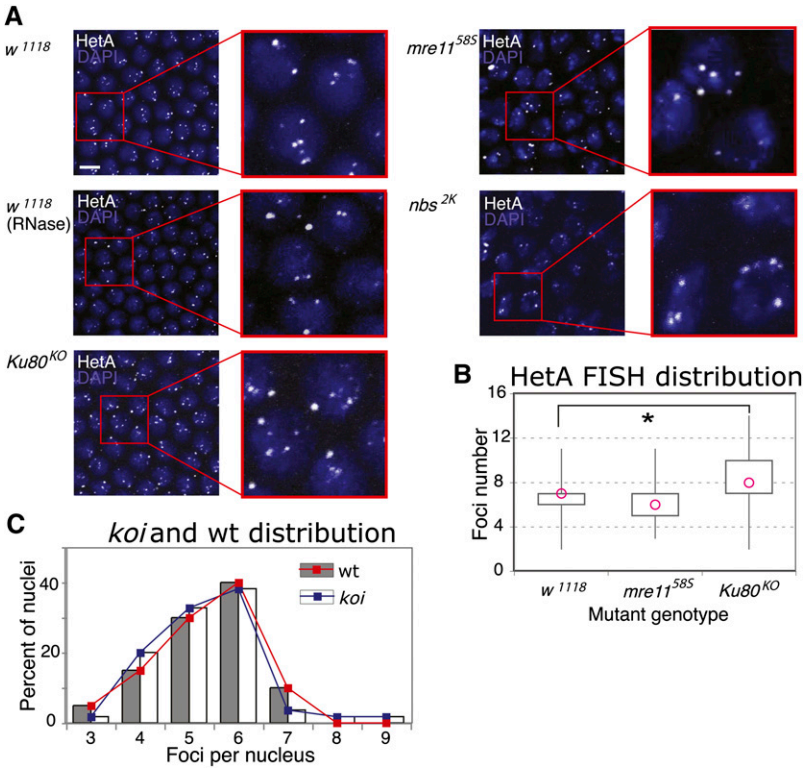

Figure 7 Candidate proteins that might mediate telomere clustering. (A) HeT-A FISH on mutant embryos, with genotypes listed on the left. Each is a confocal projection with a zoom-in, HetT-A in white, DAPI in blue. Bar for all, 5 μm. (B) Box plot of the foci-number distributions for each genotype. Pink circle: median of distribution. *x*-axis, genotypes: w^{1118} (*n* = 80 nuclei/8 embryos), $mre11^{58S}$ (*n* = 50 nuclei/5 embryos), and $Ku80^{KO}$ (*n* = 50 nuclei/5 embryos). *y*-axis: number of foci per nucleus. (C) Histogram of EGFP-HOAP foci distribution for wt embryos, represented by gray bars and red line (*n* = 20 nuclei/1 embryo), and for *koi* embryos, represented by white bars and blue line (*n* = 45 nuclei/5 embryos).

Is clustering protein mediated?

In search of potential mediators of clustering, we considered the protein component that is present at all ends. In the following sections we explore a few of the most obvious protein candidates that might mediate clustering. Because the primary stage of our analysis is the syncytial blastoderm, our genetic approach was limited to mutants that support viability. Thus, we investigated the role of the telomere maintenance complex MRN, the Ku70/Ku80 heterodimer, and a Sun-domain protein.

The MRN complex: Telomere establishment and maintenance in *Drosophila* are regulated by the repair and recombination complex MRN (Mre11/Rad50/Nbs1). Mutants that perturb the function of these regulators lead to telomere fusions that indicate cap defects (Bi *et al.* 2004, 2005; Ciapponi *et al.* 2004). Presumably MRN is important for processing telomeric DNA into substrates amenable to loading of the capping proteins (Rong 2008), although mechanistic evidence is lacking. To observe mutant effects on clustering in the embryo, we investigated the hypomorphic mutants of $mre11^{58S}$ and nbs^{2K} (Gao *et al.* 2009). Homozygotes of these hypomorphs develop to adulthood with minimal telomeric phenotypes, whereas the next-generation embryos experience extensive telomere capping failure (Gao *et al.* 2009) and provide a possibility of investigating telomere clustering within the syncytium in the absence of the MRN complex.

We used HeT-A FISH to perform counts for mutant analysis (Figure 7A). Counts were done on Z stacks without projection to avoid false colocalizations. In the wild type (w^{1118}), the distribution of telomere counts was shifted to the right in comparison to that obtained for EGFP-HOAP *in vivo*, with an average of ~6.75 foci per nucleus (SD = 1.5, 80 nuclei, eight embryos). We confirmed that the observed signal corresponded to DNA (rather than transcript), as RNase treatment of embryos prior to hybridization did not alter the FISH pattern (Figure 7A, w^{1118}/RNase).

Both *mre11* and *nbs* hypomorphs used in this study perturb the grid-like ordering of the syncytial blastoderm nuclei. However, both still show a similar pattern of FISH staining. The box plot for the distribution for the $mre11^{58S}$ hypomorph is shown in Figure 7B, with a mean of 6.22 (SD = 1.7, 50 nuclei, five embryos). The distribution is significantly smaller than the w^{1118} distribution ($P = 0.034$), but is opposite to the result expected for declustering. It is important to remember that MRN mutant embryos exhibit extensive telomere fusions. We had endeavored to focus the quantification on apparently healthy nuclei, in which chromosome integrity was presumably less affected. Nonetheless, because telomeric clustering cannot be distinguished from telomere fusions in interphase, lower numbers of telomere spots are expected in these mutants.

Ku70/80 heterodimer: The Ku70/Ku80 heterodimer is thought to have a role in clustering in *S. cerevisiae*. Ku mutants exhibit redistribution of telomeric foci from their peripheral localization to one that is more random and reduced in clustering (Laroche *et al.* 1998). For our analysis, we made a *Ku80* targeted knockout (File S1). $Ku80^{KO}$ adults are viable but

exhibit reduced female fertility. The mean for the HeT-A FISH distributions was 8.44 (SD = 2.4, n = 50, five embryos). The difference from the w^{1118} distribution was this time statistically significant (P = 0.0001). However, the distribution of a smaller count for the w^{1118} sample done side-by-side with the mutant was not significantly different (P = 0.06), indicating that there might be high variability in the FISH preparations.

Our results reveal that if Ku80 has a role in clustering in *Drosophila*, it is not the determining factor.

SUN domain protein: Mps3, a SUN-domain protein, has been implicated in telomere organization in *S. cerevisiae*, where it is presumed to be one of the components of the machinery that anchors the telomeres at the nuclear periphery (Bupp *et al.* 2007). To investigate a similar role in *Drosophila*, we inspected clustering in a mutant for the *Drosophila* SUN-domain homolog *klaroid* (*koi*) that has been implicated in nuclear migration in the developing *Drosophila* eye (Fischer *et al.* 2004; Patterson *et al.* 2004; Kracklauer *et al.* 2007). We performed quantification *in vivo* by crossing EGFP-HOAP into *koi*. As is evident from the two distributions in Figure 7C, *koi* with a mean of 5.34 foci per nucleus (SD = 1.1, n = 45, across five embryos) does not reveal altered levels of clustering compared to the wild-type EGFP-HOAP control (mean = 5.35, SD = 1.0, 20 nuclei, two embryos; P = 0.987).

Conclusions

Telomere organization in the nucleus is poorly understood. The main findings from our study are that telomere clustering in interphase is common to *Drosophila melanogaster* somatic tissues, and the numbers of clusters are consistent across at least two different cell types. This is an important finding as it confirms that clustering of telomeres is a characteristic of nuclear organization that is conserved through evolution, and it suggests that *Drosophila* is a good model for the study of clustering in higher organisms. From our investigation, it appears that there are no preferences for clustering partners among *Drosophila* telomeres. Our results clearly exclude the possibility of recombination or DNA homology as the main mediators of telomeric clustering. They rather suggest that there is an as yet unidentified component common to all telomeres, which could mediate clustering.

Our results regarding HOAP dynamics suggest increased chromatin occupancy of HOAP during interphase. We speculate that one possible explanation for the increased dynamics is that HOAP is reloaded concomitant with telomere replication. The special DNA state at the ends of chromosomes could impede replication fork progression and might require dynamic reorganization in its path. Indeed the capping protein Taz1 in *S. pombe* plays a role in replication fork progression through telomeric repeats (Miller *et al.* 2006). Further experiments are needed to determine whether HOAP could play a similar role in *Drosophila*.

Acknowledgments

We thank Min Gong for technical assistance with generating the Ku80 mutant, Lori Wallrath for providing the LacO stocks, Richa Rikhy for helpful advice on imaging live embryos, Jan Wisniewski for advice and assistance with AIP4WIN software, and Jean-Claude Walser, Robin Ngo and Jemima Barrowman for editing the manuscript.

Literature Cited

Beaucher, M., X. F. Zheng, F. Amariei, and Y. S. Rong, 2012 Multiple pathways suppress telomere addition to DNA breaks in the Drosophila germline. Genetics 191: 407–417.

Bi, X., S. C. Wei, and Y. S. Rong, 2004 Telomere protection without a telomerase; the role of ATM and Mre11 in Drosophila telomere maintenance. Curr. Biol. 14: 1348–1353.

Bi, X., M. Gong, D. Srikanta, and Y. S. Rong, 2005 Drosophila ATM and Mre11 are essential for the G2/M checkpoint induced by low-dose irradiation. Genetics 171: 845–847.

Biessmann, H., and J. M. Mason, 1988 Progressive loss of DNA sequences from terminal chromosome deficiencies in Drosophila melanogaster. EMBO J. 7: 1081–1086.

Billia, F., and U. De Boni, 1991 Localization of centromeric satellite and telomeric DNA sequences in dorsal root ganglion neurons, in vitro. J. Cell Sci. 100(Pt 1): 219–226.

Bupp, J. M., A. E. Martin, E. S. Stensrud, and S. L. Jaspersen, 2007 Telomere anchoring at the nuclear periphery requires the budding yeast Sad1-UNC-84 domain protein Mps3. J. Cell Biol. 179: 845–854.

Chikashige, Y., M. Yamane, K. Okamasa, C. Tsutsumi, T. Kojidani *et al.*, 2009 Membrane proteins Bqt3 and-4 anchor telomeres to the nuclear envelope to ensure chromosomal bouquet formation. J. Cell Biol. 187: 413–427.

Ciapponi, L., G. Cenci, J. Ducau, C. Flores, D. Johnson-Schlitz *et al.*, 2004 The Drosophila Mre11/Rad50 complex is required to prevent both telomeric fusion and chromosome breakage. Curr. Biol. 14: 1360–1366.

Daniel, A., and L. St. Heaps, 2004 Chromosome loops arising from intrachromosomal tethering of telomeres occur at high frequency in G1 (non-cycling) mitotic cells: implications for telomere capture. Cell Chromosome 3: 3.

De Lange, T., 1992 Human telomeres are attached to the nuclear matrix. EMBO J. 11: 717–724.

Dong, F., and J. Jiang, 1998 Non-Rabl patterns of centromere and telomere distribution in the interphase nuclei of plant cells. Chromosome Res. 6: 551–558.

Dubruille, R., G. A. Orsi, L. Delabaere, E. Cortier, P. Couble *et al.*, 2010 Specialization of a Drosophila capping protein essential for the protection of sperm telomeres. Curr. Biol. 20: 2090–2099.

Ferguson, M., and D. C. Ward, 1992 Cell cycle dependent chromosomal movement in pre-mitotic human T-lymphocyte nuclei. Chromosoma 101: 557–565.

Fischer, J. A., S. Acosta, A. Kenny, C. Cater, C. Robinson *et al.*, 2004 Drosophila klarsicht has distinct subcellular localization domains for nuclear envelope and microtubule localization in the eye. Genetics 168: 1385–1393.

Fujita, I., Y. Nishihara, M. Tanaka, H. Tsujii, Y. Chikashige *et al.*, 2012 Telomere-nuclear envelope dissociation promoted by Rap1 phosphorylation ensures faithful chromosome segregation. Curr. Biol. 22: 1932–1937.

Fung, J. C., W. F. Marshall, A. Dernburg, D. A. Agard, and J. W. Sedat, 1998 Homologous chromosome pairing in Drosophila

melanogaster proceeds through multiple independent initiations. J. Cell Biol. 141: 5–20.
Gao, G., X. Bi, J. Chen, D. Srikanta, and Y. S. Rong, 2009 Mre11-Rad50-Nbs complex is required to cap telomeres during Drosophila embryogenesis. Proc. Natl. Acad. Sci. USA 106: 10728–10733.
Gao, G., Y. Cheng, N. Wesolowska, and Y. S. Rong, 2011 Paternal imprint essential for the inheritance of telomere identity in Drosophila. Proc. Natl. Acad. Sci. USA 108: 4932–4937.
Gehlen, L. R., A. Rosa, K. Klenin, J. Langowski, S. M. Gasser *et al.*, 2006 Spatially confined polymer chains: implications of chromatin fibre flexibility and peripheral anchoring on telomere-telomere interaction. J. Phys. Condens. Matter 18: S245–S252.
Gotta, M., T. Laroche, A. Formenton, L. Maillet, H. Scherthan *et al.*, 1996 The clustering of telomeres and colocalization with Rap1, Sir3, and Sir4 proteins in wild-type *Saccharomyces cerevisiae*. J. Cell Biol. 134: 1349–1363.
Groth, A., A. Corpet, A. J. Cook, D. Roche, J. Bartek *et al.*, 2007 Regulation of replication fork progression through histone supply and demand. Science 318: 1928–1931.
Hiraoka, Y., D. A. Agard, and J. W. Sedat, 1990 Temporal and spatial coordination of chromosome movement, spindle formation, and nuclear envelope breakdown during prometaphase in *Drosophila melanogaster* embryos. J. Cell Biol. 111: 2815–2828.
Jansen, L. E., B. E. Black, D. R. Foltz, and D. W. Cleveland, 2007 Propagation of centromeric chromatin requires exit from mitosis. J. Cell Biol. 176: 795–805.
Kracklauer, M. P., S. M. Banks, X. Xie, Y. Wu, and J. A. Fischer, 2007 Drosophila klaroid encodes a SUN domain protein required for Klarsicht localization to the nuclear envelope and nuclear migration in the eye. Fly (Austin) 1: 75–85.
Laroche, T., S. G. Martin, M. Gotta, H. C. Gorham, F. E. Pryde *et al.*, 1998 Mutation of yeast Ku genes disrupts the subnuclear organization of telomeres. Curr. Biol. 8: 653–656.
Levis, R. W., 1989 Viable deletions of a telomere from a Drosophila chromosome. Cell 58: 791–801.
Li, Y., J. R. Danzer, P. Alvarez, A. S. Belmont, and L. L. Wallrath, 2003 Effects of tethering HP1 to euchromatic regions of the Drosophila genome. Development 130: 1817–1824.
Manuelidis, L., 1984 Different central nervous system cell types display distinct and nonrandom arrangements of satellite DNA sequences. Proc. Natl. Acad. Sci. USA 81: 3123–3127.
McKee, B. D., 2004 Homologous pairing and chromosome dynamics in meiosis and mitosis. Biochim. Biophys. Acta 1677: 165–180.
Mellone, B. G., K. J. Grive, V. Shteyn, S. R. Bowers, I. Oderberg *et al.*, 2011 Assembly of Drosophila centromeric chromatin proteins during mitosis. PLoS Genet. 7: e1002068.
Miller, K. M., O. Rog, and J. P. Cooper, 2006 Semi-conservative DNA replication through telomeres requires Taz1. Nature 440: 824–828.
Molenaar, C., K. Wiesmeijer, N. P. Verwoerd, S. Khazen, R. Eils *et al.*, 2003 Visualizing telomere dynamics in living mammalian cells using PNA probes. EMBO J. 22: 6631–6641.
Nagele, R. G., A. Q. Velasco, W. J. Anderson, D. J. McMahon, Z. Thomson *et al.*, 2001 Telomere associations in interphase nuclei: possible role in maintenance of interphase chromosome topology. J. Cell Sci. 114: 377–388.
Palladino, F., T. Laroche, E. Gilson, A. Axelrod, L. Pillus *et al.*, 1993 SIR3 and SIR4 proteins are required for the positioning and integrity of yeast telomeres. Cell 75: 543–555.
Patterson, K., A. B. Molofsky, C. Robinson, S. Acosta, C. Cater *et al.*, 2004 The functions of Klarsicht and nuclear lamin in developmentally regulated nuclear migrations of photoreceptor cells in the Drosophila eye. Mol. Biol. Cell 15: 600–610.
Pierron, G., and F. Puvion-Dutilleul, 1999 An anchorage nuclear structure for telomeric DNA repeats in HeLa cells. Chromosome Res. 7: 581–592.
Ramirez, M. J., and J. Surralles, 2008 Laser confocal microscopy analysis of human interphase nuclei by three-dimensional FISH reveals dynamic perinucleolar clustering of telomeres. Cytogenet. Genome Res. 122: 237–242.
Rong, Y. S., 2008 Telomere capping in Drosophila: dealing with chromosome ends that most resemble DNA breaks. Chromosoma 117: 235–242.
Ruault, M., A. De Meyer, I. Loiodice, and A. Taddei, 2011 Clustering heterochromatin: Sir3 promotes telomere clustering independently of silencing in yeast. J. Cell Biol. 192: 417–431.
Scherf, A., J. J. Lopez-Rubio, and L. Riviere, 2008 Antigenic variation in Plasmodium falciparum. Annu. Rev. Microbiol. 62: 445–470.
Scherthan, H., 2001 A bouquet makes ends meet. Nat. Rev. Mol. Cell Biol. 2: 621–627.
Schober, H., V. Kalck, M. A. Vega-Palas, G. Van Houwe, D. Sage *et al.*, 2008 Controlled exchange of chromosomal arms reveals principles driving telomere interactions in yeast. Genome Res. 18: 261–271.
Schuh, M., C. F. Lehner, and S. Heidmann, 2007 Incorporation of Drosophila CID/CENP-A and CENP-C into centromeres during early embryonic anaphase. Curr. Biol. 17: 237–243.
Silva-Sousa, R., E. López-Panadès, and E. Casacuberta, 2010 Drosophila telomeres: an example of co-evolution with transposable elements. Genome Dyn. 7: 46–67.
Sullivan, W., M. Ashburner, and R. S. Hawley, 2000 *Drosophila Protocols*, Cold Spring Harbor Laboratory Press, Cold Spring Harbor, NY.
Taddei, A., and S. M. Gasser, 2004 Multiple pathways for telomere tethering: functional implications of subnuclear position for heterochromatin formation. Biochim. Biophys. Acta 1677: 120–128.
Taddei, A., G. Van Houwe, S. Nagai, I. Erb, E. Van Nimwegen *et al.*, 2009 The functional importance of telomere clustering: global changes in gene expression result from SIR factor dispersion. Genome Res. 19: 611–625.
Vourc'h, C., D. Taruscio, A. L. Boyle, and D. C. Ward, 1993 Cell cycle-dependent distribution of telomeres, centromeres, and chromosome-specific subsatellite domains in the interphase nucleus of mouse lymphocytes. Exp. Cell Res. 205: 142–151.
Weipoltshammer, K., C. Schofer, M. Almeder, V. V. Philimonenko, K. Frei *et al.*, 1999 Intranuclear anchoring of repetitive DNA sequences: centromeres, telomeres, and ribosomal DNA. J. Cell Biol. 147: 1409–1418.

Communicating editor: C.-ting Wu

GENETICS

Supporting Information
http://www.genetics.org/lookup/suppl/doi:10.1534/genetics.113.155408/-/DC1

Clustering and Protein Dynamics of *Drosophila melanogaster* Telomeres

Natalia Wesolowska, Flavia L. Amariei, and Yikang S. Rong

DOI: 10.1534/genetics.113.155408

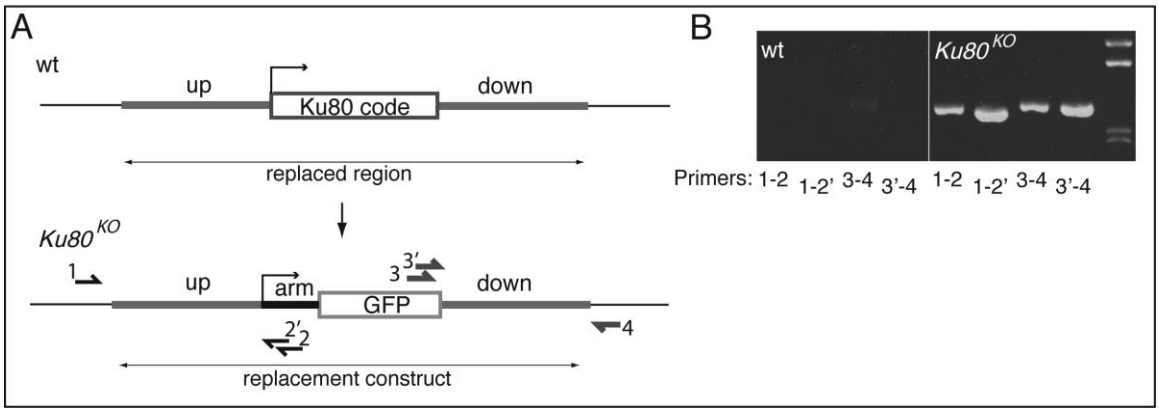

Figure S1 Molecular characterization of Ku80 deletion

A. Schematics of Ku80 region. Top: the wt Ku80 region with upstream (up) and downstream (dn) sequences (~2.5 kb each) that flank the coding region; "replacement region" designates sequences replaced by ends-out targeting. Bottom: the Ku80 region in Ku80Δ mutant; the up and dn flanking fragments were used in ends-out gene targeting, in which the Ku80 coding sequence was replaced by an arm-GFP marker gene; "replacement construct" designates sequences brought in by ends-out targeting. The flanking sequences are unaltered from wt. Half-arrows indicate primers used for the PCRs in B. Note that primer 1 and 4 reside outside the Ku80 region. Primers 2 and 2' reside within armadillo promoter sequences, while primer 3 and 3' are within GFP.

B. PCR products from four test PCRs for wt and Ku80Δ lines. Primer pairs used for each PCR are indicated bellow the image, and their locations are specified within the schematic in A. For exact primer sequences see the Supplemental Methods.

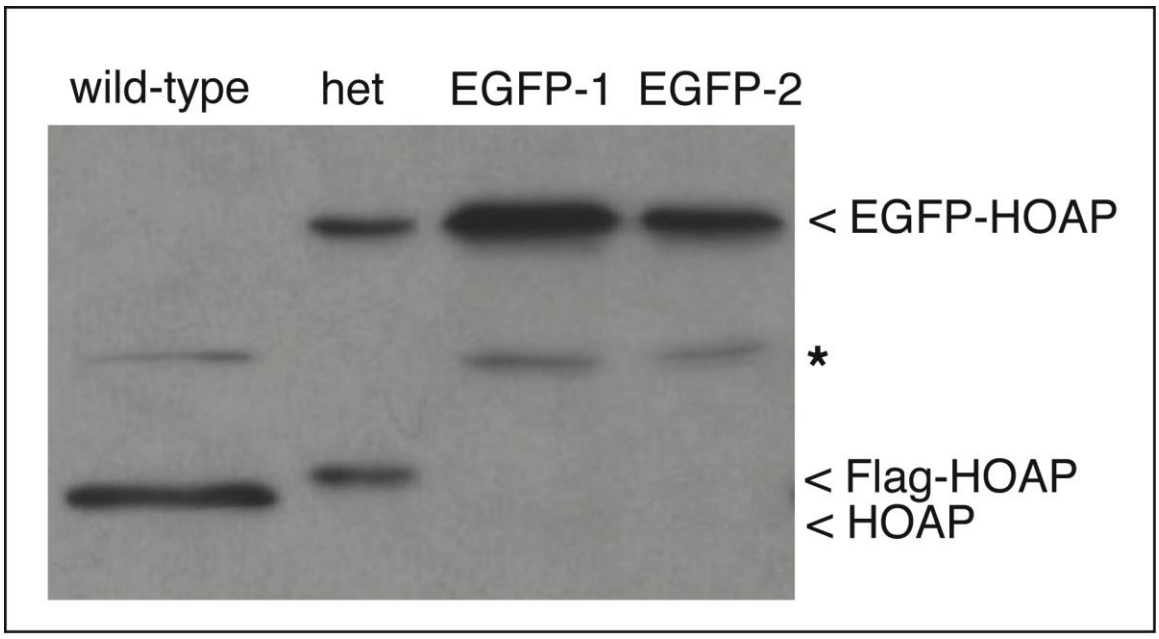

Figure S2 EGFP-HOAP is produced at normal level
Western Blot was performed on embryos extracts from flies of the indicated genotype and probed using rabit anti-HOAP antibody. Lanes are labeled at the top: 1) wild-type; 2) het: heterozygous line, which carries both EGFP-HOAP and a Flag-tagged HOAP (accounting for slightly larger HOAP band); 3) EGFP-1 and EGFP-2: two independent EGFP-HOAP lines which carry only the tagged version of HOAP. The major band corresponds to a cumulative size of HOAP plus EGFP. A non-specific band is labeled with an asterisk (*).

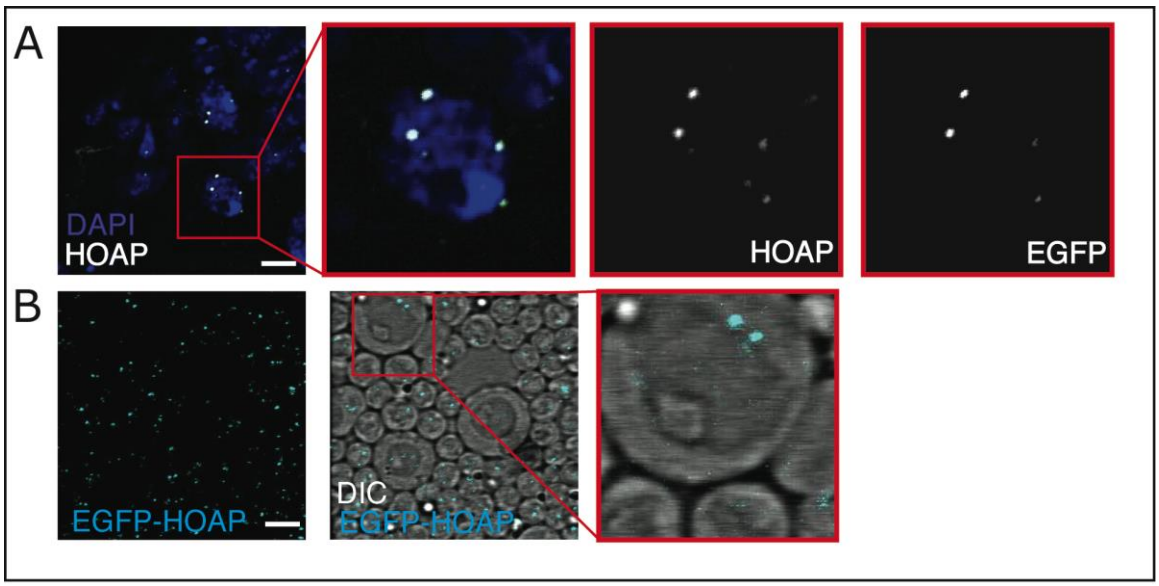

Figure S3 Telomere distribution in larval brain

A. Confocal projection showing immunostaining in larval brain nuclei; HOAP or EGFP in white as indicated, DAPI in blue. Panels in order: 1st, merge; 2nd, zoom-in of area in red square; 3rd, HOAP antibody staining alone for zoom-in; 4th, EGFP fluorescence alone for zoom-in.

B. Confocal projections collected from live larval brain; EGFP in cyan, DIC in grayscale. Panels in order: 1st, EGFP alone; 2nd, DIC and EGFP; 3rd, zoom-in of the area in the red square.

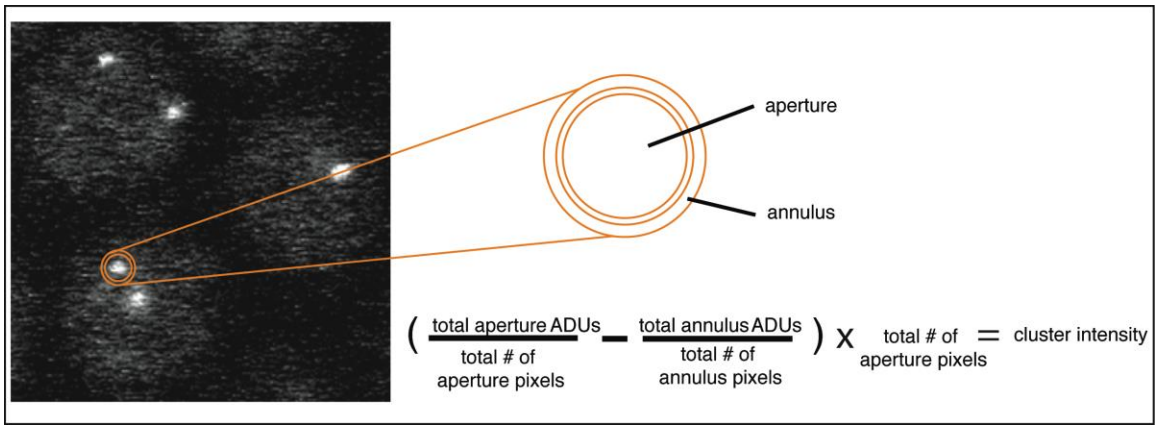

Figure S4 The measurement method used to quantify EGFP-HOAP signal in embryos
A schematic of an aperture superimposed over a Z-section. Aperture is the area of the inner circle, whereas annulus is the area of the surrounding ring. The measurement of spot intensity is obtained according to the formula presented, i.e. the average pixel intensity within the aperture was adjusted for background by subtracting average pixel intensity within the annulus and then multiplying by the number of aperture pixels.

File S1

Supporting Methods

Generating the construct for Ku80 replacement

Vector pBS(arm-GFP), previously described in Gong et al. (2005) was used for generating the construct for Ku80 replacement. A 2.5 kb fragment immediately upstream of the start codon of Ku80 was PCR-amplified and cloned into the HindIII and KpnI sites in pBS(arm-GFP). A 2.5 kb fragment downstream of the stop codon of Ku80 was PCR-amplified and cloned into the NotI and XbaI sites in pBS(arm-GFP). The final 7.8 kb targeting fragment that contained the Ku80-upstream and downstream fragments as well as the arm-GFP marker was cloned into the NotI and XhoI sites of the ends-out targeting vector pW30, which carries the white+ (w+) marker gene (Gong and Golic, 2003). Primers used for the test PCRs on targeted lines (see Supplemental Figure 1): 1– Ku80-2394d - CAGAGACCCACTCACAAATG, 2 – arm288up - CGATAACTCCTCTATCGCAG, 2' – arm31up-GCAGTCGTAGAAGTGGGTTC, 3 – eGFP-1269f - GACAACCACTACCTGAGCAC, 3'– eGFP1330f - CACATGGTCCTGCTGGAGTTC, 4 – Ku80-10334u - GTAAGCAGTTACAATGCCATCAC.